

An Adaptive MLSE Receiver for TDMA Digital Mobile Radio

RENATO D'AVELLA, LUIGI MORENO, SENIOR MEMBER, IEEE, AND MARCELLO SANT'AGOSTINO

Abstract—The European Telecommunications Administrations (CEPT) have recently defined the standard for the Pan-European public land mobile system. It is based on digital voice coding and TDMA access structure with a bit rate of 270.8 kbits/s and a Gaussian MSK modulation. This paper presents the simulation study of an adaptive receiver, based on the concept of maximum likelihood sequence estimation (MLSE), which compensates for the heavy selective distortions caused by multipath propagation.

The receiver includes a matched filter and a modified Viterbi processor and is suitable to be implemented in a digital form. It operates adaptively, in a training mode at the beginning of each burst, as well as in a tracking mode during message detection. This makes the receiver robust both to fast Doppler shifts and to a large frequency offset. Simulation results are presented which show the performance in different multipath environments, with echo delay in excess of 20 μ s and vehicle speed up to 250 km/h. Such results have been evaluated using the propagation channel models defined by CEPT experts on the basis of field tests. The adaptive receiver is presently being implemented in the Italtel laboratories.

I. INTRODUCTION

A digital land mobile radio system is presently being standardized by the European PTT Administrations (CEPT), to be operated in the 900 MHz frequency band. This system will provide a unified standard for a foreseen market of some million subscribers, in place of the different analog systems actually used in Europe. The main characteristics, relevant to the transmission system, are the use of a time division multiple access (TDMA) scheme, with a gross bit rate of about 270 kbits/s and Gaussian minimum shift keying (GMSK) modulation.

This paper addresses the radio transmission problems caused by the multipath fading which require the use of a sophisticated adaptive receiver. Some digital equalizer structures have been studied at Italtel [1], [2] and a hardware implementation for a MLSE receiver based on the Viterbi algorithm is being carried on for a transmission experiment [3].

The present simulation study shows the expected performance for such a receiver in the presence of the main channel impairments and disturbances. In Section II, some basic descriptions of the system structure and transmission assumptions are given. Section III and Section IV, respectively, describe the MLSE receiver structure and

the receiver adaptation procedures. Finally, in Section V, simulation results are reported.

II. SYSTEM ASSUMPTIONS

A description of the whole system is out of the scope of the present paper. The receiver design, as presented in the following sections, only needs some basic data concerning the digital transmission structure and the adaptability requirements. These have been established in a meeting of European Telecommunications Administrations experts and successively adjusted along with the progress of the works [4].

A. Transmission Characteristics

A time division multiple access (TDMA) scheme is assumed, with eight speech channels on the same RF carrier.

Both the base and the mobile stations transmit a sequence of message bursts, located in the assigned time slots. The transmitted burst (Fig. 1) includes a preamble, known at the receiver, whose function is to allow an estimate of the channel impulse response (CIR) and a proper initialization of the receiver parameters, on a burst-by-burst basis.

A Gaussian minimum shift keying (GMSK) modulation has been adopted, with a relative bandwidth factor equal to 0.3. This type of signal belongs to the class of continuous phase modulations (CPM) [5] that can be approximated as binary offset QAM signals and can be detected by a quadrature coherent demodulator.

In the proposed implementation, quadrature demodulation is adopted but no carrier coherency is requested to the receiver. Also, the sampling phase of the demodulated in-phase and quadrature signals is not bound to a definite position with respect to the symbols.

Only a coarse synchronization (a time window about 20–30 percent wider than the burst duration) and a reduction of the receiver frequency offset below 1 kHz are assumed. These conditions are achieved during the start-up procedure by detecting some dedicated bursts on the control channel. This problem is not discussed in the present work.

The gross bit rate is $R = 1/T = 270.8$ kbits/s, that comes from a 75 percent redundancy for the error correcting codes plus the necessary overhead (preamble, guard time, etc.). Anyway, the channel coding gain is not considered in the following analysis.

Manuscript received January 8, 1988; revised September 20, 1988.
R. D'Avella and M. Sant'Agostino are with ITALTEL SIT, 20019 Settimo Milanese, Italy.
L. Moreno is at Via Asti 10, 10131 Torino, Italy.
IEEE Log Number 8824961.

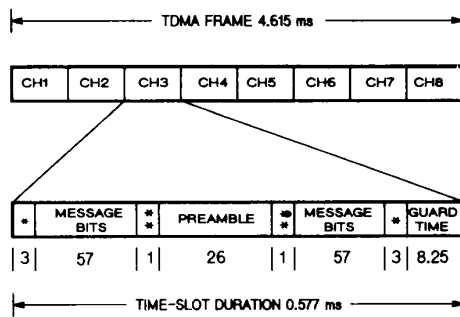


Fig. 1. TDMA frame and burst structure of the GSM system [4]: (*) tail bits, (**) housekeeping bits.

B. Adaptability Requirements

The receiver must be able to compensate for the heavy selective distortions due to the multipath propagation. Echo delays up to 15–20 μ s, which correspond to about 4–5 bit periods, can be expected in mountainous areas [6]. To allow a comparison of performance results, some typical echo patterns have been selected by a group of propagation experts [7]. Up to six main echo paths are assumed, with uncorrelated Rayleigh distributed amplitudes and Doppler spectra. Therefore, at each message burst, during the “training mode” of adaptive operation, the receiver has to estimate the channel response and to configure itself appropriately.

An additional improvement can be obtained by the receiver adaptability during the message detection (“tracking mode”). This could be necessary to cope with very fast channel response variations, in case of high speed of the mobile, and to compensate for the phase error due to the residual frequency offset of the receiver.

Our present objective for such a phase adjustment is to achieve an acceptable operation with a residual frequency error of ± 1 kHz. As shown in Section V, this can also provide a simple way of correcting the local oscillator frequency, thus reducing the frequency offset nearly to zero.

III. MLSE RECEIVER STRUCTURE

Under severe channel distortions, the use of nonlinear equalization is advisable [8], [9]. A preliminary work on candidate techniques [1], [2], also taking into account the constraints on implementation complexity, led to the choice of an MLSE receiver as appropriate for the present application. More specifically, the receiver structure proposed by Ungerboeck [10] has been considered, which includes a matched filter (MF) and a modified Viterbi processor. The Ungerboeck receiver is suitable to be applied to any QAM coherent demodulator and is attractive for a number of reasons.

- It does not require a whitening filter (as in Forney’s receiver [11]), since the modified Viterbi processor takes into account the correlation of (nonwhitened) noise samples.

- The metrics computation, as defined in the modified

Viterbi processor, does not require any squaring operation.

- It is suitable to be implemented in an adaptive form.

The block diagram in Fig. 2 shows a digital implementation of the MLSE Ungerboeck receiver, which will be discussed in the present work. After demodulation and low-pass filtering of the received signal, the baseband components $x(t)$ and $y(t)$, are sampled and A/D converted, with a sampling frequency equal to the bit rate. Then the signal samples are filtered through a digital N -tap transversal filter, which approximates the MF response.

Theoretically, the use of a MF makes the receiver insensitive to the carrier and clock phases, respectively, used to demodulate and to sample the received signal, provided that the MF coefficients are properly adjusted and the time span of the MF is long enough to include all the channel impulse responses.

To this end, the number of taps N in the MF must be chosen to comply with the maximum echo delays which are expected to be observed in the operational environment. Additionally, it must be taken into account that the modulator output pulses are spread over about three bit periods. As a result, the value $N = 6$ seems to be advisable in order to be able to operate with most of the multipath profiles to be found in actual operating conditions. The MF output samples are finally processed according to the modified Viterbi algorithm, which operates on a number of states $S = 2^{N-1}$. This means, as already known, that the Viterbi processor complexity is an exponential function of N . A summary of the metrics computation formula is given in [2], as specialized to a binary offset-QAM signal. It is shown that the computational load in the Viterbi processor is limited to about $4 \cdot S$ additions for each received bit, while real number multiplications are avoided.

IV. ADAPTATION PROCEDURES

A. Training Mode

A new estimate of the CIR is obtained at each received burst by correlating the received signal with the preamble bit sequence, which is known at the receiver. The CIR estimate includes all the selective elements of the transmission system (modulator pulse shaping, propagation selective distortions, and receiver analog filter).

According to the GSM specifications, the 26 bit preamble sequence is formed by a 16 bit word plus 5 cyclically repeated bits at each end, for protection purposes. Eight different preamble sequences have been selected by optimizing the autocorrelation and crosscorrelation properties.

The CIR estimate is truncated at N samples by considering the N bit time span where the maximum energy is concentrated. Finally, the MF tap gains can be directly computed as the complex conjugates of the estimated CIR samples.

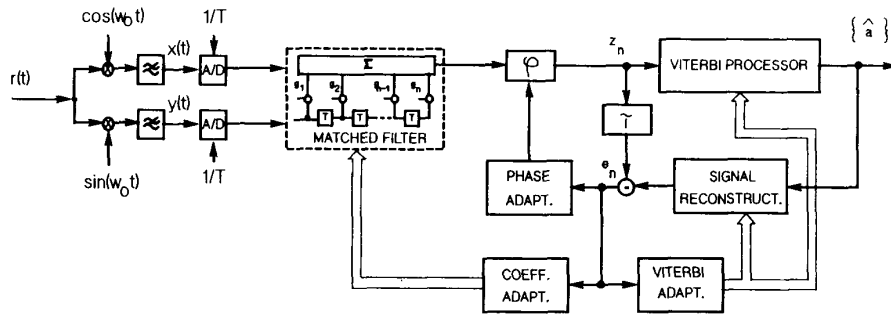


Fig. 2. Block diagram of the MLSE adaptive receiver.

B. Tracking Mode

The channel variations during the message transmission can be compensated by the adaptation loops shown in Fig. 2 by adjusting the MF tap gains, the Viterbi processor parameters, and the signal phase. In practice, there are two independent adaptation functions: a tracking of the CIR variations and a tracking of the phase variations.

The feedback loops are driven by the error sample sequence $e(n)$, which is computed by comparing the signal sample $z(n)$ at the Viterbi processor input with a replica of the same signal sample based on the detected symbol sequence and on the estimated channel response.

It is worthwhile noting that a delay in the estimation of the symbol sequence (and consequently in the error sample computation) is caused by the Viterbi processor. This represents a limit in the tracking performance of the adaptive receiver. The phase adaptation, as shown in Fig. 2, is performed immediately before the Viterbi processor in order to minimize the overall loop delay. To improve the phase error compensation, a second-order loop has been adopted; a typical performance is shown in Fig. 3 where the frequency offset during the burst can be estimated from the end-to-end phase difference.

In the CIR tracking procedure, a gradient algorithm is used, as suggested in [10], to minimize the mean-square error by adjusting the MF tap gains and the Viterbi processor parameters. This function has shown a noticeable performance improvement in a previous study [2] where the preamble was assumed to be at the beginning of the burst. However, with the present burst structure (preamble in the middle of the burst, Fig. 1) the CIR tracking seems to be less useful.

C. Adaptability Versus Receiver Complexity

The adaptation procedures obviously increase the processing load, so a compromise must be reached between adaptability and receiver complexity. This applies mainly to the CIR tracking function, while the phase tracking is easier.

If the CIR estimate could be assumed to be constant for the whole burst (no CIR tracking), then the transition metrics would be computed only once in a given burst. On the other hand, when the CIR variations are assumed fast enough (or the message duration long enough) not to allow a quasi-static channel assumption, the Viterbi pro-

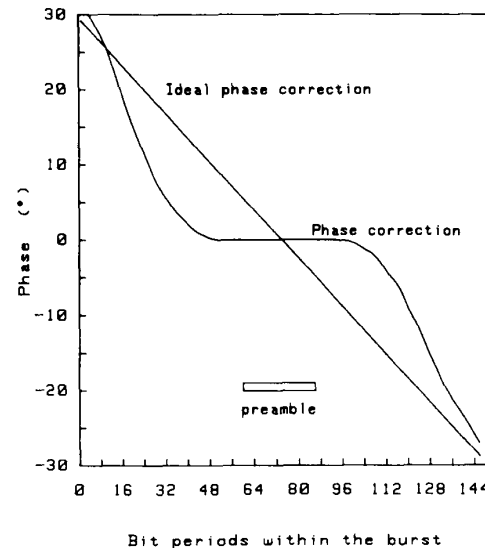


Fig. 3. Example of phase adaptation behavior with a 300 Hz frequency offset in the absence of noise and distortions.

cessor parameters would have to be computed every few bits.

The merit of the Viterbi processor presently considered is that the metrics computation requires only four additions/state/bit. This allows the CIR tracking mode of operation to be implemented at an acceptable cost in terms of receiver complexity.

V. SIMULATED PERFORMANCE

A computer simulation program has been set up in order to evaluate the performance of a TDMA mobile radio system with the proposed MLSE receiver. The simulated model reflects the structure shown in Fig. 2. A 32-state Viterbi receiver ($N = 6$) has been adopted, according to the previous considerations.

A seven-pole Butterworth receiving filter has been considered, with a 3-dB bandwidth (two-sided) equal to $0.75R$.

The simulated channel impairments are: flat Gaussian noise or flat Rayleigh fading with Doppler frequency shift or multiple echoes as discussed below. Co-channel or adjacent-channel interferences and receiver frequency-offset are also considered. In evaluating the simulation results, reference will be made to a BER = 0.01 only as a com-

parison point. In practice, due to the channel coding gain, not considered here, the acceptable performance for the speech channel could be achieved with BER up to about 0.05.

A. Static Channel Performances

The error rate performance in the absence of channel distortions is shown in Fig. 4, as a function of the (energy per bit)/(noise spectral density) ratio E_b/N_0 .

About 1 dB degradation is exhibited at $\text{BER} = 0.01$ in comparison to an ideal QPSK or MSK coherent system. Part of this degradation is typical of GMSK with optimum coherent parallel detection [12], while an additional impairment is caused by the noisy estimate of the CIR.

The sensitivity to co-channel and adjacent channel interference has been also evaluated in the absence of channel distortions. The channel spacing is 200 kHz. Fig. 5 shows the BER as a function of the C/I ratio. As far as the co-channel interference is considered, the useful signal preamble is assumed to be interfered by a signal modulated by a random sequence.

B. Performances Under Dynamic Fading

In a first set of simulation runs, the dynamic behavior of the mobile radio channel has been simulated by means of a simple two-ray model, with a variable delay τ between the two rays. Both the direct and the delayed signal components are independently Rayleigh faded, with equal average power, and frequency shifted with a Doppler spread related to the given vehicle speed [13].

Some examples of the error rate versus the signal-to-noise ratio E_b/N_0 are given in Fig. 6 where both simulations and some experimental results (with the prototype reported in [3]) are shown.

With $\tau = 0 \mu\text{s}$, the channel model is equal to a flat Rayleigh channel. The performance improvement with $\tau = 10 \mu\text{s}$ shows that a "time diversity" benefit is gained by using the ML estimation scheme. As long as the MF response closely approximates the channel response, this can be achieved. With increasing echo delays, this condition is no longer satisfied and the error rate is expected to grow.

The effectiveness of the 32-state MLSE receiver with long echo delays is investigated in Fig. 7 where BER versus τ is reported for given E_b/N_0 values. The time diversity gain is maximum in the range $2 \mu\text{s} < \tau < 12 \mu\text{s}$, while for $\tau > 20 \mu\text{s}$, a significant degradation is observed. All the above results assume a 50 km/h vehicle speed.

Additional simulations have been performed with more complex echo patterns, selected by the COST Propagation Group [7], as representative of urban (TU), rural (RA), and hilly (HT) environments (Fig. 8). Again, each signal component is independently Rayleigh faded with average power given by the selected pattern, and Doppler spread [13].

The error rate versus E_b/N_0 is reported in Fig. 9. For the rural area model, where the effect of the mobile speed is also shown, the results can be considered as a worst

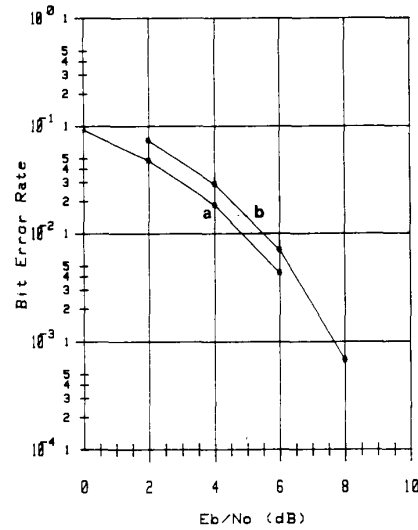


Fig. 4. Bit error rate in the AWGN channel: (a) ideal channel response estimate, (b) noisy channel response estimate.

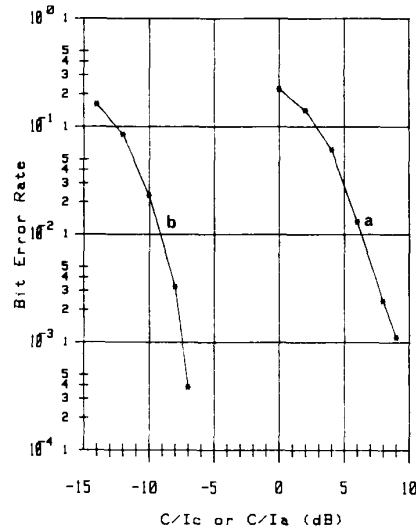


Fig. 5. Bit error rate in a static channel with interference: (a) co-channel interference, (b) adjacent channel interference (channel spacing 200 kHz).

case because the use of Rayleigh fading assumes no significant direct path. The impairment due to co-channel interference in the urban environment is presented in Fig. 10; as a comparison, the performance with a static channel is reported as well.

As a general comment from the above results, we observe that the performance with the COST echo patterns is consistent with the results on the two-ray channel, which can be a much simpler test tool for laboratory measurements. The objective of satisfactory operation with delays up to 15–20 μs can be achieved by the 32-state MLSE receiver.

C. Receiver Frequency Offset

The receiver frequency offset was included in the simulated model in order to evaluate the effectiveness of the

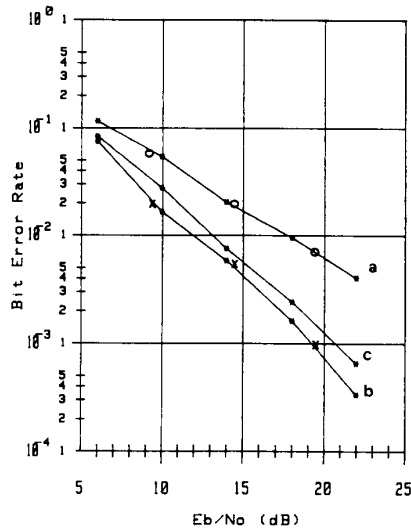


Fig. 6. Bit error rate in a two-ray Rayleigh channel. Simulation results: (a) echo delay $\tau = 0 \mu s$, (b) $\tau = 10 \mu s$, (c) $\tau = 16 \mu s$. Experimental results [3]: (o) $\tau = 0 \mu s$, (x) $\tau = 10 \mu s$.

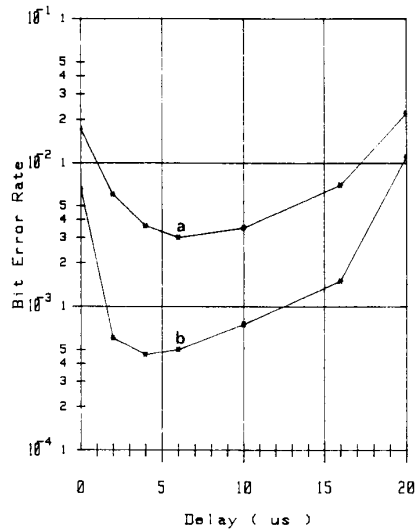
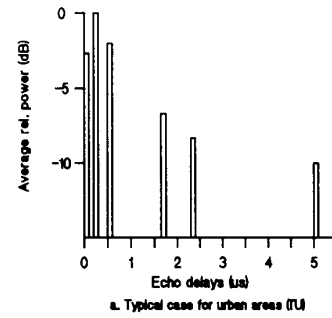


Fig. 7. Bit error rate in a two-ray Rayleigh channel as a function of echo delay: (a) $E_b/N_0 = 10 \text{ dB}$, (b) $E_b/N_0 = 20 \text{ dB}$.

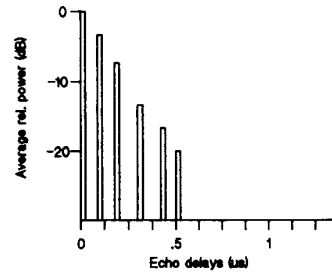
phase adaptation loop and of the frequency offset estimation and compensation process.

Fig. 11 shows the error rate as a function of the frequency offset Δf for a two-ray channel model ($\tau = 10 \mu s$, 50 km/h). Clearly, in the absence of any phase adaptation, a severe degradation is observed for offset values of a few hundreds hertz ($\Delta f = 500 \text{ Hz}$ means an overall 50° phase shift from the preamble midpoint to the burst edge). It can be seen that the phase adaptation extends the operating range, with an acceptable performance impairment, up to about 1 kHz frequency offset.

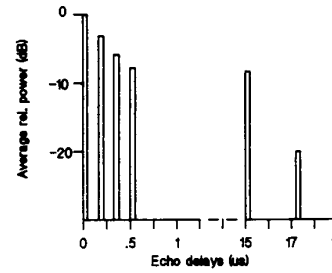
It is interesting to examine the distribution of bit errors within the received burst, with a relatively large frequency offset with and without phase compensation (Fig. 12).



a. Typical case for urban areas (TU)



b. Typical case for rural areas (RA)



c. Typical case for Hilly Terrain (HT)

Fig. 8. Typical echo patterns chosen as representative of different environments [7].

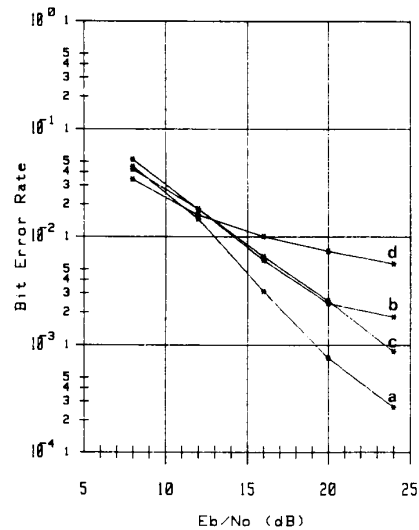


Fig. 9. Bit error rate in a Rayleigh channel with echo patterns as in Fig. 8: (a) TU with vehicle speed 50 km/h, (b) RA, 100 km/h, (c) HT, 100 km/h, (d) RA, 250 km/h.

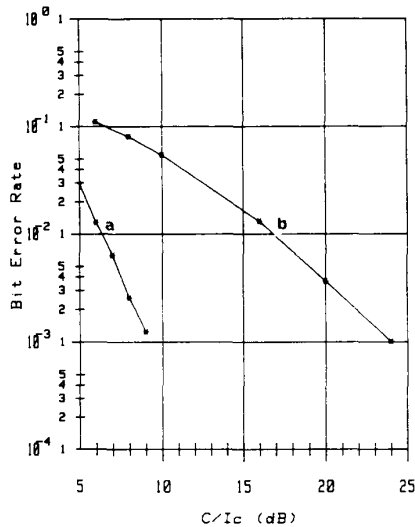


Fig. 10. Bit error rate with co-channel interference: (a) static channel, (b) TU, 50 km/h.

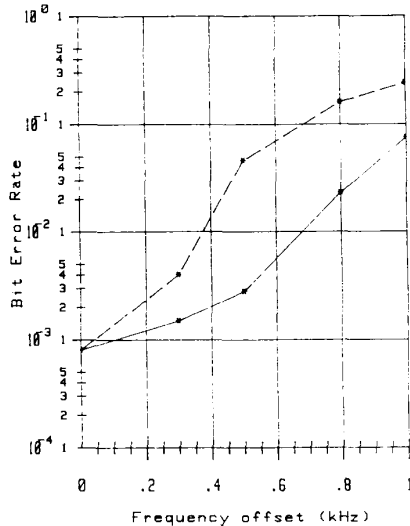


Fig. 11. Bit error rate as a function of receiver frequency offset, with (—) and without (---) phase adaptation for a two-ray Rayleigh channel, $\tau = 10 \mu\text{s}$, 50 km/h, $E_b/N_0 = 20 \text{ dB}$.

The ML estimation of the received sequence has been applied also to the preamble bits, not considering that they are known to the receiver, to evaluate an error rate that could be used for monitoring purposes. It can be noticed that the preamble bit errors are much less than in the message, due to the better channel estimate available. In the two message parts, the errors, without phase adaptation [Fig. 12(a)], grow continuously when moving towards the burst edges, while with phase adaptation [Fig. 12(b)], the error rate is maintained almost constant throughout the message. In both cases, it can be noticed that the BER on the preamble is the same because in that region the phase adjustment cannot work (see Fig. 3). Besides the minimization of the error rate, the phase adaptation function provides also, within each burst, an estimate $\hat{\Delta f}$ of the

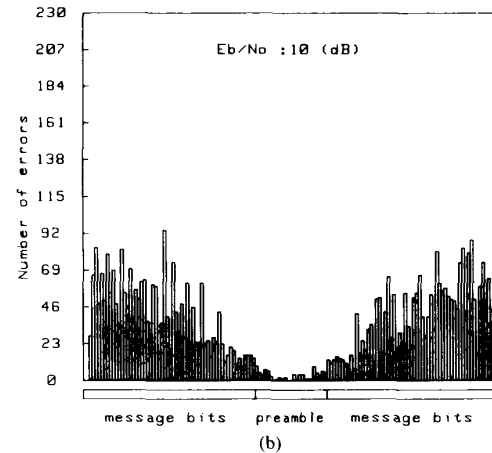
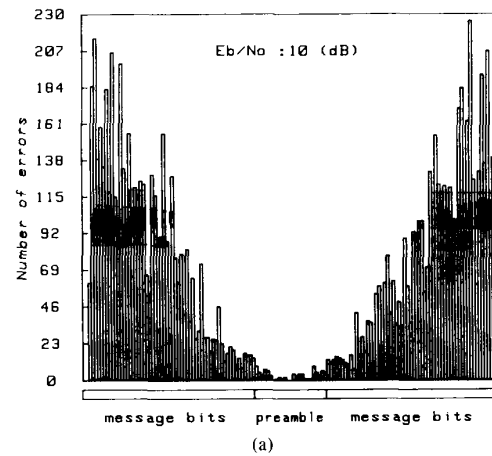


Fig. 12. Error patterns throughout the burst with a frequency offset of 800 Hz; two-ray Rayleigh channel, $\tau = 10 \mu\text{s}$, 50 km/h, $E_b/N_0 = 10 \text{ dB}$. (a) Without phase adaptation: BER (message) = 0.19, BER (preamble) = 0.011. (b) With phase adaptation: BER (message) = 0.09, BER (preamble) = 0.011.

receiver frequency offset which can be used to correct the receiver VCO frequency. Fig. 13 shows two examples of statistical distributions of the estimated frequency error, with two different signal-to-noise ratios (10 and 20 dB) in dynamic fading conditions. Such estimates are affected by a bias, which leads to underestimating the actual frequency offset. However, this does not represent a serious drawback, since a step-by-step procedure can be used to compensate for the overall frequency offset, as shown by the example in Fig. 14.

In this example, the estimated frequency offset $\hat{\Delta f}$ is averaged over 100 time slots (about 0.5 s); then the VCO frequency is adjusted with multiples of a 50 Hz step. The residual frequency offset is again estimated with the same procedure and this allows a fast convergence of the compensation process up to less than 50 Hz.

It must be noted that the $\pm 1 \text{ kHz}$ range covered by the digital receiver using the phase adaptation function described before corresponds to about 1 ppm frequency in-

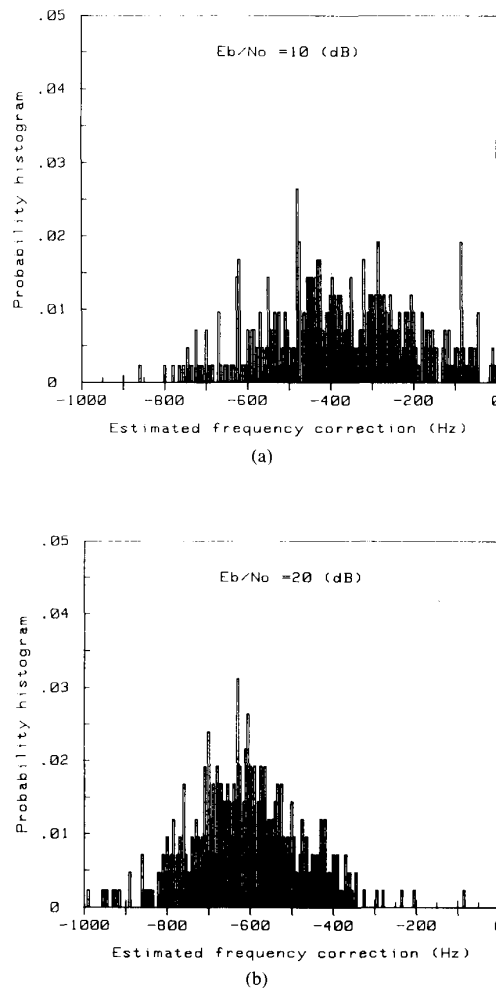


Fig. 13. Histogram of estimated frequency correction, with a frequency offset of 800 Hz, same channel as in Fig. 12: (a) $E_b/N_0 = 10$ dB (average frequency comp.: -400 Hz), (b) $E_b/N_0 = 20$ dB (average frequency comp.: -650 Hz).

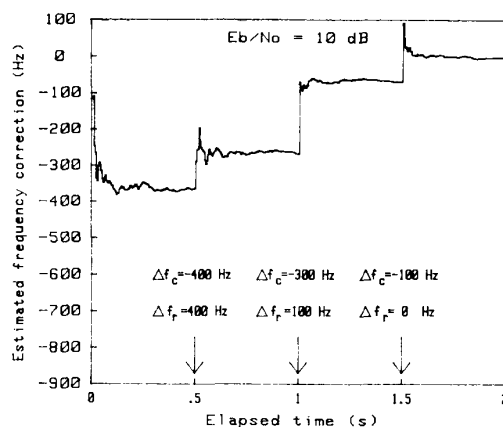


Fig. 14. Running average of the estimated frequency correction as a function of elapsed time, same channel as in Fig. 12 and in Fig. 13, with initial frequency offset of 800 Hz and $E_b/N_0 = 10$ dB. Every 0.5 s the averaged frequency correction is applied and the running average is reset (Δf_c = frequency correction; Δf_r = residual frequency offset).

stability at the mobile receiver (with a much better stability at the base station). This can be achieved by a coarse frequency correction procedure, for example, from ± 10 kHz to ± 1 kHz, made possible by the system control structure and not discussed here.

VI. CONCLUSIONS

A coherent orthogonal receiver for GMSK signals has been discussed, whose decision process is based on maximum likelihood sequence estimation. The receiver structure includes a matched filter and a 32-state modified Viterbi processor and is suitable for a digital adaptive implementation. The complexity of the modified Viterbi processor is significantly reduced and no real number multiplication or squaring operation is needed. This allows an update of channel estimates from bit to bit, in order to cope with fast Doppler fading and large frequency offsets.

The simulation results show the ability of the proposed receiver to operate in a multipath environment with echo delays of the order of 20 μ s and vehicle speeds in excess of 200 km/h (like in the case of high-speed trains). In particular, the phase adaptability during the message reception has been shown to provide remarkable advantages. A prototype receiver based on the above design features is presently being implemented and the first results match the simulations quite well.

Even if the motivation of the study and the numerical results are related to the present European developments, the adaptive MLSE receiver discussed above is applicable to several CPM modulations and its use also can be considered in other contexts.

The paper has been focused on transmission aspects relevant to the reception of a single burst. Related problems are to be considered in the context of a burst sequence transmission and cellular operation (like quality estimation, power control, hand-over criteria, etc.). Further investigations are being performed on these topics.

REFERENCES

- [1] R. D'Avella, L. Moreno, and M. Sant'Agostino, "Adaptive equalization in TDMA mobile radio system," presented at VTC 1987, Tampa, FL, May 1987.
- [2] R. D'Avella and L. Moreno, "Maximum likelihood adaptive techniques in the digital mobile radio environment," presented at the Int. Conf. Digital Land Mobile Radio Commun., Venezia, Italy, June 1987.
- [3] A. Colamonico *et al.*, "Italian experimental activity on the land mobile GSM system," presented at the 3rd Nordic Seminar Digital Land Mobile Radio Commun., Copenhagen, Denmark, Sept. 1988.
- [4] A. Maloberti, "Definition of the radio subsystem for the GSM Pan-European digital mobile communications system," presented at the Int. Conf. Digital Land Mobile Radio Commun., Venezia, Italy, June 1987.
- [5] C. E. Sundberg, "Continuous phase modulation," *IEEE Commun. Mag.*, vol. 24, pp. 25-28, Apr. 1986.
- [6] E. Damosso, "Wide-band propagation measurements at 900 MHz," *Alta Frequenza*, vol. 57, pp. 65-74, Feb.-Mar. 1988.
- [7] "Proposal on channel transfer functions to be used in GSM tests late 1986," COST 207 TD(86)51.
- [8] J. G. Proakis, *Digital Communications*. New York: McGraw-Hill, 1983, ch. 6.
- [9] E. Eleftheriou and D. D. Falconer, "Adaptive equalization techniques for HF channels," *IEEE J. Select. Areas Commun.*, vol. SAC-5, pp. 238-247, Feb. 1987.

- [10] G. Ungerboeck, "Adaptive maximum-likelihood receiver for carrier-modulated data-transmission systems," *IEEE Trans. Commun.*, vol. COM-22, pp. 624-636, May 1974.
- [11] G. D. Forney, "Maximum-likelihood sequence estimation of digital sequence in the presence of intersymbol interference," *IEEE Trans. Inform. Theory*, vol. IT-18, pp. 363-378, May 1972.
- [12] M. S. El-Tanany and S. A. Mahmoud, "Mean-square error optimization of quadrature receivers for CPM with modulation index $1/2$," *IEEE J. Select. Areas Commun.*, vol. SAC-5, pp. 896-905, June 1987.
- [13] W. C. Jakes, *Microwave Mobile Communications*. New York: Wiley, 1974.



Renato D'Avella received the Dr. Ing. degree in electronics engineering from the Politecnico di Torino, Italy, in 1980.

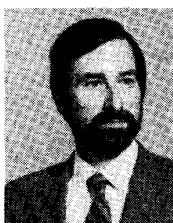
After military service in the Technical Services of the Italian Army, he joined ITALTEL SIT, Milan, Italy, where he works in the Research and Development Laboratories. He was involved in the analysis of modulation methods suitable for digital land mobile system and interference evaluation in cellular structures. Currently he works on the development of computer simulations of narrow-band TDMA systems.



Luigi Moreno (M'78-SM'86) was born in Torino, Italy, on July 15, 1949. He received the Dr. Ing. degree in electronics engineering from the Politecnico di Torino, Torino, in December 1972.

From 1973 to 1982 he was with the Centro Studi e Laboratori Telecomunicazioni (CSELT), Torino, where his activity was mainly devoted to research projects on digital radio systems for both terrestrial and satellite applications. In 1982 he joined GTE Telecomunicazioni, Italy, where he was involved in the design and field testing of high capacity digital radio-relay systems. Since 1985 he has worked as an independent consultant. His main interests are in the fields of digital radio communications, adaptive countermeasures for multipath fading channels, and simulation techniques for transmission systems analysis.

Since 1974 Dr. Moreno has attended several CCIR meetings (Study Groups 1 and 9) as a member of the Italian delegation. He is a member of AEI (Italian Electrical and Electronic Association).



Marcello Sant'Agostino received the Dr. Ing. degree in electronics engineering from the Politecnico di Torino, Italy, in 1963.

From 1965 to 1978 he was with the Centro Studi e Laboratori Telecomunicazioni (CSELT), Torino, the research and study center of the Italian telecommunications group STET. As a head of the Radio Relay System Section, he was engaged in system engineering studies on digital radio links, and in computer simulation activities. He was active in the international standardization works

(CCIR). In 1978 he joined ITALTEL Research and Development Laboratories where he is now head of the Cellular Engineering Group, with responsibility for the activities of the digital land mobile system project.